Quaternary Research 81 (2014) 181–188

Contents lists available at ScienceDirect

Quaternary Research

journal homepage: www.elsevier.com/locate/yqres

Trace-element variations in an annually layered stalagmite as recorders of climatic changes and anthropogenic pollution in Central China

Liangcheng Tan [a,*], Chuan-Chou Shen [b], Yanjun Cai [a], Li Lo [b], Hai Cheng [c], Zhisheng An [a]

[a] State Key Laboratory of Loess and Quaternary Geology, Institute of Earth Environment, Chinese Academy of Sciences, Xi'an 710075, China
[b] High-precision Mass Spectrometry and Environment Change Laboratory (HISPEC), Department of Geosciences, National Taiwan University, Taipei 10617, Taiwan
[c] Institute of Global Environmental Change, Xi'an Jiaotong University, Xi'an 710049, China

ARTICLE INFO

Article history:
Received 29 September 2013
Available online 28 December 2013

Keywords:
Annually layered stalagmite
Trace elements
REE geochemistry
Climate change
Environmental pollution
Central China

ABSTRACT

We analyzed variations in the Sr/Ca, Ba/Ca, REE/Ca (REE: rare earth element), Zn/Ca, and Pb/Ca ratios preserved in an annually layered stalagmite, XL21, from central China. The stalagmite record spans the 95 year period AD 1914–2008. The Sr/Ca and Ba/Ca ratios have a significant positive correlation with the stalagmite's growth rate, suggesting that they were primarily controlled by growth-rate variations. Variations in REE/Ca ratios are consistent with local temperature changes, suggesting temperature influenced REE concentrations in the stalagmite over decadal to annual timescales. Higher temperature in this humid area can increase vegetation cover, microbial activity, and organic decomposition in the soil, resulting in enhanced pCO_2, organic matter concentration and reduced pH, and consequently increased REE mobilization from the overlying soil layer and host rock. Higher temperatures may also increase the natural Zn mobilization from the overlying soil mediated by organic matter and consequently may have led to increased Zn retention in XL21. An increasing trend is seen in the Pb/Ca ratios from XL21 since 1985, which is consistent with increased lead production in this area, and indicates an increase in mine-derived lead pollution in the local environment over the past 30 years.

© 2013 University of Washington. Published by Elsevier Inc. All rights reserved.

Introduction

Cave speleothems are ideal for reconstructing past climatic and environmental changes because they often grow continuously, yield data at a high temporal resolution, can be accurately dated, and suffer little secondary alteration (e.g., McDermott, 2004; Fairchild et al., 2006). Studies of stable isotopes ($\delta^{18}O$, $\delta^{13}C$) preserved in speleothems from the Asian monsoon region have achieved great success in recent years (e.g., Wang et al., 2001, 2005, 2008; Fleitmann et al., 2003; Yuan et al., 2004; Cheng et al., 2009; Cai et al., 2012). However, trace-element signatures preserved in speleothems are not commonly used, and have received less attention than the stable isotope approach. Nevertheless, it has been demonstrated that trace elements incorporated into the calcium carbonate matrix (e.g., Mg, Sr, Ba, Y, P, and U) reflect past climate variability (Fairchild and Treble, 2009, and references therein). For example, Mg variations in a modern stalagmite from southwestern Australia were suggested to be an effective palaeohydrological indicator in this region on annual timescales, while Sr, Ba, and Na were suggested to depend on growth rate (Treble et al., 2003). Mg/Ca and Sr/Ca ratios in a stalagmite from southern Brazil varied in tandem with $\delta^{18}O$ during the last glacial period, and were explored as a proxy for changes in local rainfall recharge over millennial timescales (Cruz et al., 2007). Richter et al. (2004) first analyzed rare earth elements (REE) in stalagmites from Germany, and suggested that their enrichment reflected periods of more intense weathering, which usually correspond to warm and humid conditions. Another study, from central China, also showed that speleothem REE were enriched during interstadials, but became depleted during stadial periods, confirming that more intense weathering and more dynamic hydrology under warm and humid climates favor the enrichment of REE in stalagmites (Zhou et al., 2008). These latter two studies highlight the potential for using REE series preserved in speleothems to reconstruct past climate change.

With the development of the mining, smelting, and metal-treating industries, heavy metal pollution in China has become increasingly serious, and now poses a severe threat to both humans and the environment in some regions (e.g., Chen et al., 1999; Cheng, 2003). There is an increasing need to reconstruct the environmental pollution history in China to assist current environmental monitoring. Speleothems have the potential to preserve environmental pollution signals derived from the overlying soil layers (Frisia et al., 2005). In contrast to the mobility of pollutants in dendrochemical records, element mobility is not usually a problem for speleothems, except where aragonite is converted to calcite after deposition (Fairchild and Treble, 2009). Recently, Siklosy et al. (2011) provided the first successful example of using the chemical composition of a stalagmite to reconstruct the history of environmental pollution, in this case, related to U ore mining in Hungary.

In this study, we analyze variations in the Sr/Ca, Ba/Ca, REE/Ca (i.e., La/Ca, Ce/Ca, Pr/Ca, Nd/Ca, Sm/Ca, Eu/Ca, Gd/Ca, Tb/Ca, Dy/Ca, Ho/Ca, Er/Ca, Tm/Ca, Yb/Ca, and Lu/Ca), Zn/Ca, and Pb/Ca ratios over the period

* Corresponding author.
E-mail addresses: tanlch@ieecas.cn, tlch1209@163.com (L. Tan).

0033-5894/$ – see front matter © 2013 University of Washington. Published by Elsevier Inc. All rights reserved.
http://dx.doi.org/10.1016/j.yqres.2013.12.001

https://doi.org/10.1016/j.yqres.2013.12.001 Published online by Cambridge University Press

AD 1914–2008 preserved in an annually layered stalagmite (XL21) from central China. We present direct comparisons between the trace-element records and the observed temperature and precipitation records, and discuss the main factors controlling the trace-element variations.

Cave location and sample description

Xianglong Cave (33°00′N, 106°20′E; 940 m above sea level at the entrance) is located on the southern flank of the Qinling Mountains in central China (Fig. 1). In summer, the Asian summer monsoon brings warm humid air and causes substantial monsoon rainfall at the site (>70% of the annual rainfall, Liu et al., 2003). During winter, the Siberian–Mongolian High and westerly winds maintain cold and dry conditions, and carry airborne dust from the Gobi Desert and drylands in northwestern China to the site (Wei et al., 2000). There are two lead mines 10–16 km northwest of Xianglong Cave (Fig. 1), and lead mining and smelting has taken place in the area for the past 30 years. The present-day mean annual air temperature and precipitation in this area are 13°C and 1100 mm, respectively. For data on monthly rainfall and temperature variations, see Tan et al. (2013).

The cave has a relatively thick roof (~100 m) and its known length exceeds 1.2 km; the humidity of the inner chambers is around 100%. Recharge to the karst aquifer above the cave is likely to be derived from meteoric precipitation (Tan et al., 2013). As a result of water storage in the relatively thick cave roof, infiltration is continuous even during the driest winter months. An active stalagmite (XL21), which was 4.2 cm long, was collected about 700 m from the entrance of Xianglong Cave in October 2009 (Fig. 1). The supplying dripwater entry was about 8 m above the sample site. A vertical section through the stalagmite (Fig. 2) shows regular laminae that alternate from dark, compacted layers (DCL) to white, porous layers (WPL). Here, we study the uppermost 2.9 cm of XL21, which is composed of pure aragonite, as revealed by X-ray diffraction analysis (Tan et al., 2013).

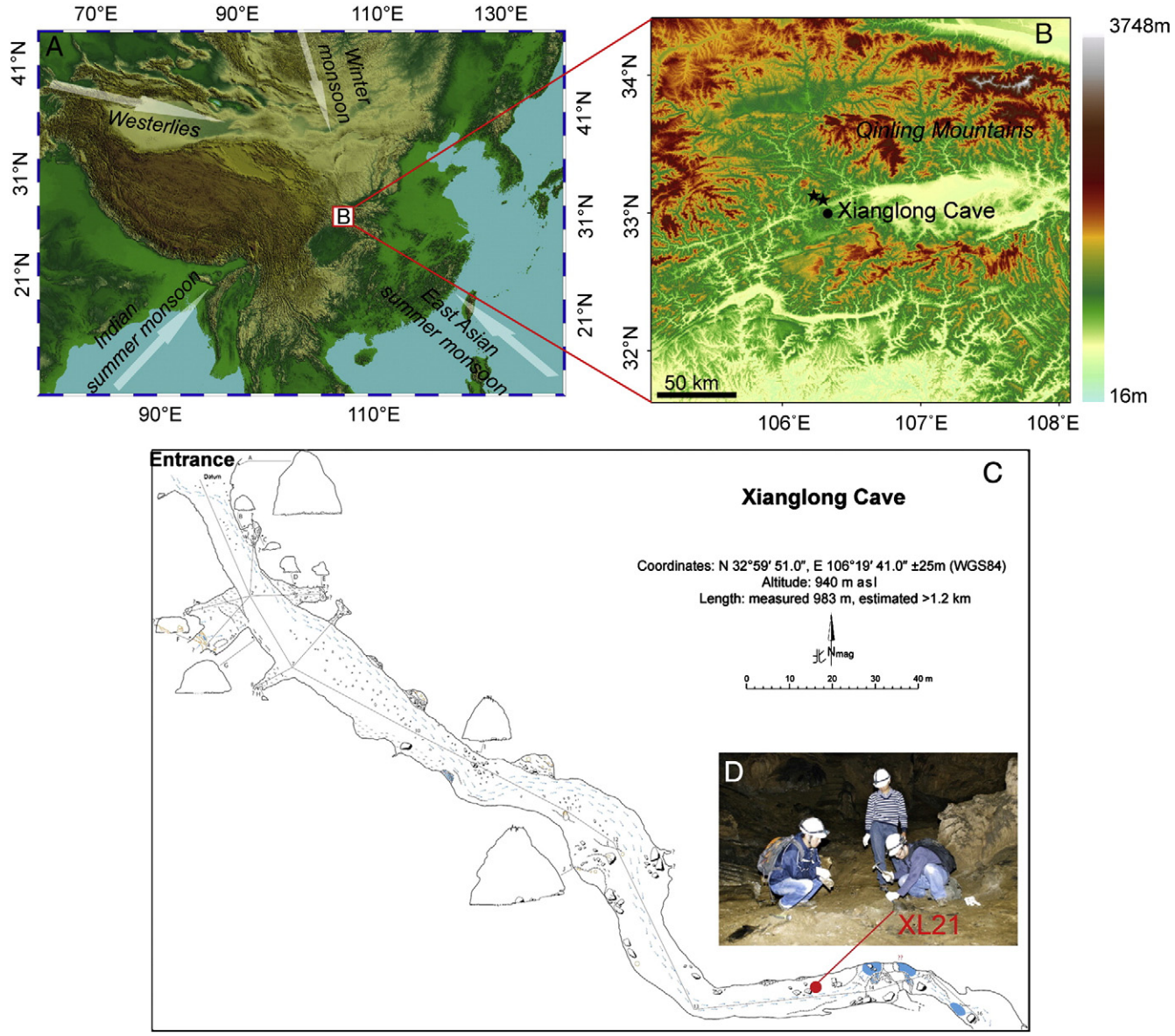


Figure 1. Location and plan view of Xianglong Cave. (A) Overview map showing the study region. Arrows indicate the directions of the East Asian summer monsoon, Indian summer monsoon, East Asian winter monsoon, and westerlies. (B) Enlarged regional topographic map showing the locations of Xianglong Cave (black dot), two lead mines (black stars), and the Qinling Mountains. Topographic GTOPO30 data are from the USGS EROS Center (Earth Resources Observation and Science Center: http://eros.usgs.gov/#/Find_Data/Products_and_Data_Available/gtopo30_info). (C) Plan view of Xianglong Cave. (D) Photograph showing the sampling site of stalagmite XL21 in the cave.

https://doi.org/10.1016/j.yqres.2013.12.001 Published online by Cambridge University Press

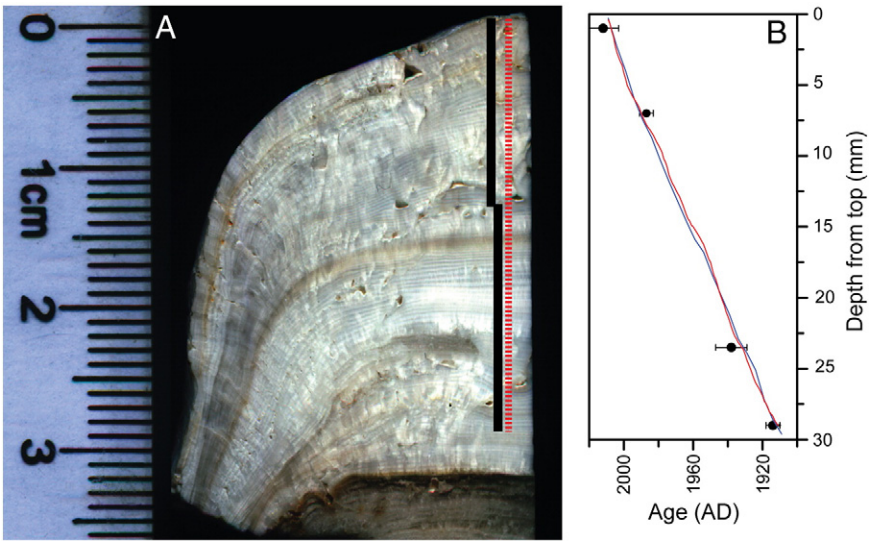


Figure 2. (A) Section through stalagmite XL21 showing micromilling paths (thick black lines) for C/O isotopic analysis and drilling path for trace element analysis (red dashed line). (B) Comparison of age models based on visible annual layers (blue line), annual $\delta^{18}O$ cycles (red line), and ^{230}Th dates (solid circles with errors).

Methods

A hand-held carbide dental drill, with a 0.9-mm diameter drill bit, was used to recover subsamples (50–100 mg powder) along the growth axis for ^{230}Th dating (Edwards et al., 1987; Shen et al., 2012; Cheng et al., 2013). The measurements were performed using a multi-collector inductively coupled plasma mass spectrometer (MC-ICPMS) (Shen et al., 2012; Cheng et al., 2013) at the Isotope Laboratory of the University of Minnesota, USA. We scanned the polished surface of the stalagmite and counted the visible laminae in images viewed using the Adobe Photoshop program. To obtain the annual cycles preserved in the $\delta^{18}O$ variability within the stalagmite, we performed stable isotope analysis at increments of 50 μm using the micromill sampling method (McDermott, 2004). The stable isotopes were analyzed using an online, automated carbonate preparation system (Kiel III) linked to a Finnigan MAT-252 gas-source mass spectrometer at the Institute of Earth Environment (Chinese Academy of Sciences), Xi'an, China. Replicate sample runs showed that the two-sigma precision of the $\delta^{18}O$ analysis was better than 0.1‰. An accurate chronology was then constructed based on $\delta^{18}O$ cycle counting (see Tan et al., 2013 for details).

To analyze the variations of the Sr/Ca, Ba/Ca, Zn/Ca, Pb/Ca, and REE/Ca ratios in the stalagmite, we used the rapid standard-bracketing method, which was developed to measure femtogram levels of trace elements in natural carbonate samples by ICPMS and does not require any chemical separation steps (Shen et al., 2011). Subsamples of 2–4 mg were drilled along the growth axis of XL21 at an interval of 0.5–1.0 mm, and dissolved in 5% ultrapure HNO_3. One in-house matrix-matched standard, STD20, was gravimetrically prepared with superpure calcium carbonate powder and the corresponding trace element solution standard to calculate the concentration of trace elements in the stalagmite (Shen et al., 2011; Lo et al., 2013).

To attenuate the matrix effect of Ca^{2+} concentration on accurate elemental ratio determination, dissolved Ca^{2+} in both sample and standard aliquots was adjusted to the same level (20 ppm) prior to measurement. A natural stalagmite standard, WYS, was also prepared. Both the laboratory standard and the stalagmite standard were used to assess analytical reproducibility. Trace element analysis was performed at the High-Precision Mass Spectrometry and Environment Change Laboratory (HISPEC) at National Taiwan University, Taiwan using a Finnigan Element II ICP-MS. The detailed chemical procedures, instrumentation, and calibration used are described in Shen et al. (2011) and Lo et al. (2013). The replicates show that the two-sigma precision was 0.5% for Sr/Ca, 0.8% for Ba/Ca, 1.5% for Zn/Ca, 5% for Pb/Ca, and 2%–6% for REE/Ca.

Results

The high-resolution $\delta^{18}O$ record contained 98 cycles, which is consistent with the visible laminae counts and within the error of the ^{230}Th dates, indicating that the visible layers and $\delta^{18}O$ cycles are annual (Fig. 2). Detailed $\delta^{18}O$ and ^{230}Th dating results are described in Tan et al. (2013). We used the $\delta^{18}O$ cycles obtained from XL21 to construct the age–depth model (see Tan et al., 2013 for details) for the trace element series, and developed a biennial-resolution trace element series from 1914 to the present day (October 2009; i.e., the time of sampling).

The Sr/Ca ratio preserved in stalagmite XL21 varied between 0.318 and 0.407 mmol/mol, while the Ba/Ca ratio was in the range 0.101–0.142 mmol/mol. The average concentration of the total REE/Ca (ΣREE/Ca) was ~90 nmol/mol, and ranged from 54 to 267 nmol/mol. The Zn/Ca ratio varied between 0.127 and 0.362 mmol/mol. A remarkable increasing trend in the Pb/Ca series was observed in the uppermost 8 mm of the stalagmite. The trace-element series show broad similarities with each other during the growth period of XL21, except for the anomalously increasing trend of the Pb/Ca ratios in the uppermost part of the stalagmite (Fig. 3).

Discussion

Controls on Sr and Ba variations in XL21

There is a significant positive correlation between the stalagmite Sr/Ca and Ba/Ca records, with a correlation coefficient of 0.89 ($N = 48$, $p < 0.01$). Variations in Sr and Ba levels in stalagmites usually show significant positive correlations over seasonal to millennial timescales (e.g., Roberts et al., 1998; Finch et al., 2001; Johnson et al., 2006; Hori et al., 2013), indicating their common controlling factors (Fairchild and Treble, 2009). Previous studies have suggested that multiple factors affect Sr and Ba variations in speleothems. These factors include: different sources (i.e., aeolian particles, dry and wet atmospheric deposition, bedrock, superficial sediment deposits, and inorganic soil constituents); different types of flow paths; varying amounts of water–rock interaction; the temperature- and growth-rate-dependent partition coefficients for Sr (D_{Sr}) and Ba (D_{Ba}) between water and carbonate,

https://doi.org/10.1016/j.yqres.2013.12.001 Published online by Cambridge University Press

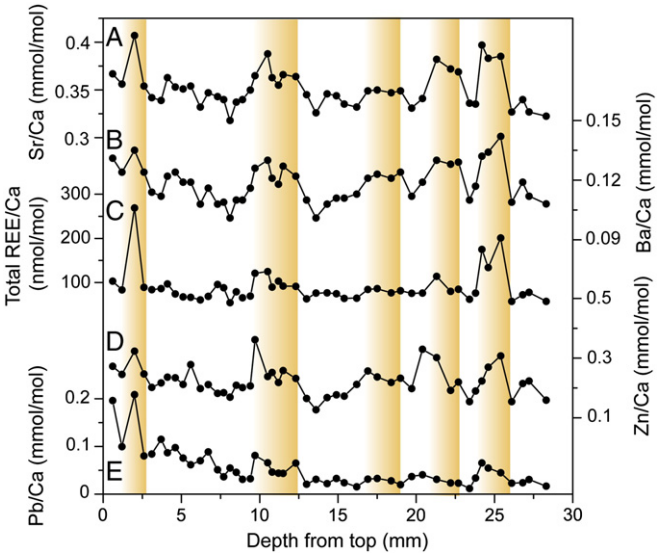


Figure 3. Results of trace-element analysis of stalagmite XL21. (A) Sr/Ca. (B) Ba/Ca. (C) ΣREE/Ca. (D) Zn/Ca. (E) Pb/Ca. The trace-element series are broadly similar during the growth period of XL21 (dark yellow bars), except for the anomalous increasing trend of the Pb/Ca ratio in the uppermost section of the stalagmite.

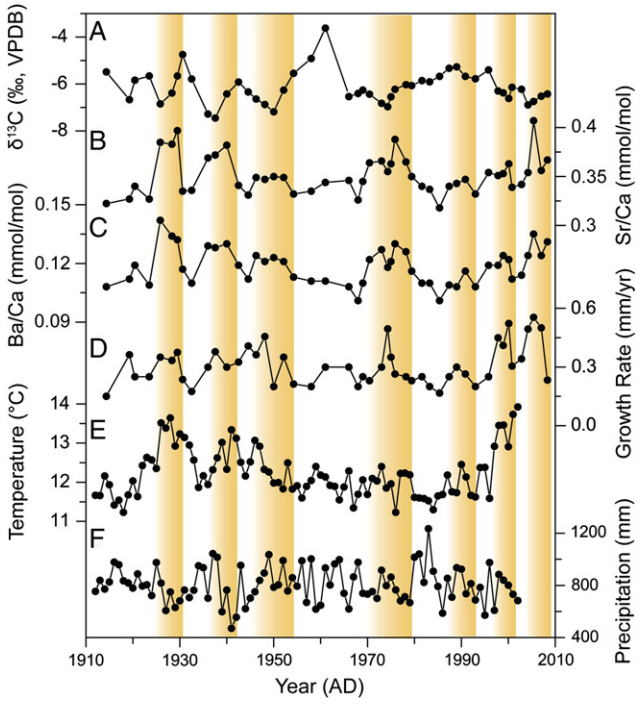


Figure 4. Comparison of proxy records of (A) $\delta^{13}C$, (B) Sr/Ca, (C) Ba/Ca, and (D) growth rate of stalagmite XL21 with CRU TS2.1 grid data for (E) annual temperature and (F) precipitation in the Xianglong Cave area. Although the values of temperature and precipitation in the Xianglong Cave area during the past 50 yr are slightly underestimated by the CRU datasets, their variations are well modeled. The correlation coefficients are about 0.7 at a significance level of 99%, between the CRU data and observed temperature and precipitation records during the period AD 1957–2002. The dark yellow bars mark periods showing good agreement among the different records, except for precipitation record.

respectively; and the variable extent of prior calcite precipitation (PCP) (Fairchild and Treble, 2009; Wong et al., 2011, and references therein). The primary controlling factor may differ in each cave and speleothem.

Numerous studies have suggested that the primary sources of Ca, Sr, and Ba in speleothems from caves located far from the sea are the bedrock and overlying regolith (Fairchild and Treble, 2009; Bourdin et al., 2011, and references therein), despite some exceptions (Goede et al., 1998; Ayalon et al., 1999; Zhou et al., 2009). The extent of any water–rock interaction is largely dictated by the variable water residence time, which is closely related to the rainfall amount outside the cave (Musgrove and Banner, 2004; Wong et al., 2011). There was no significant correlation between the Sr/Ca and Ba/Ca ratios in XL21, and local rainfall amounts (data from the CRU TS2.1 grid dataset), suggesting that water–rock interaction was not the primary controlling factor (Fig. 4).

The climate in the area of Xianglong Cave is a Cwa climate, and the plentiful rainfall here is unfavorable to PCP (Karmann et al., 2007). As the values of D_{Sr} and D_{Ba} are much less than 1, PCP would cause an increase in the Sr/Ca and Ba/Ca ratios in water and carbonate (Fairchild et al., 2006; Fairchild and Treble, 2009). In this case, progressive CO_2 degassing could also lead to the increase of $\delta^{13}C$ in solution and carbonate due to the preferential loss of ^{12}C in degassed CO_2 (McDermott, 2004), which would in turn lead to significant positive correlations between Sr/Ca, Ba/Ca, and $\delta^{13}C$ in the stalagmite (Johnson et al., 2006; Cruz et al., 2007; Hori et al., 2013). Figure 4 indicates that variations in the $\delta^{13}C$ record (the $\delta^{13}C$ series was interpolated to the chronology of the trace elements series) of XL21 are out of phase with the Sr/Ca and Ba/Ca records, with a significant negative correlation coefficient of −0.41 between Sr/Ca and $\delta^{13}C$, and −0.49 between Ba/Ca and $\delta^{13}C$ ($N = 48$, $p < 0.01$; Fig. 5). These results suggest that PCP was not the main factor controlling Sr/Ca and Ba/Ca variations in XL21.

In contrast, the pattern of Sr/Ca and Ba/Ca variations in XL21 closely matches changes in the growth rate (Tan et al., 2013; the growth-rate series was interpolated to the chronology of the trace-element series). For example, the Sr/Ca and Ba/Ca ratios increased when the growth rate was high in the late 1920s, 1930s, 1940s, 1980s, 1990s, and also the mid-1970s and mid-2000s. The Sr/Ca and Ba/Ca ratios decreased during periods of low growth rate, such as from the late 1950s to the 1960s, and the early 1980s (Fig. 4). The correlation coefficient between Sr/Ca and growth rate is 0.46 ($N = 48$, $p < 0.01$), and between Ba/Ca and growth rate is 0.47 ($N = 48$, $p < 0.01$; Fig. 5). These results suggest that the Sr and Ba variations in XL21 were controlled mainly by growth-rate variations, supporting the previous conclusions from experimental studies (Lorens, 1981; Tesoriero and Pankow, 1996) and speleothem studies (e.g., Roberts et al., 1998; Huang and Gong, 2001; Treble et al., 2003, 2005; Stoll et al., 2012).

As temperature was the primary factor controlling growth-rate variability in XL21 via its influence on the production of CO_2 in the soil overlying the cave (see Tan et al., 2013 for details), it could also have had an indirect effect on the variations in Sr and Ba levels (Roberts et al., 1998). In addition, high temperatures likely increased vegetation cover and biological activity, leading to higher concentrations of carbonic acid. As a result, increased leaching of soil cations and carbonate dissolution would have occurred, resulting in the enhancement of Sr/Ca and Ba/Ca in the speleothem (Fairchild et al., 2000; Hellstrom and McCulloch, 2000). This inference is supported by good agreement among the Sr/Ca and Ba/Ca series and the temperature variations (Fig. 4; data from CRU TS2.1 grid dataset).

Controls on REE variations in XL21

To attempt to determine the climatic significance of the REE variations in XL21, we first investigated potential source changes of the REE. There are two sources of REE in XL21: the overlying soil layer and the limestone host rock (Zhou et al., 2012). Different sources may have different REE signatures. Figure 6 shows that the host limestone-normalized REE patterns of XL21 did not change significantly throughout the stalagmite growth period, which was characterized by heavy REE-enrichment with negative Ce and positive Eu values. The consistent REE patterns throughout XL21 indicate steady contributions of REE from

https://doi.org/10.1016/j.yqres.2013.12.001 Published online by Cambridge University Press

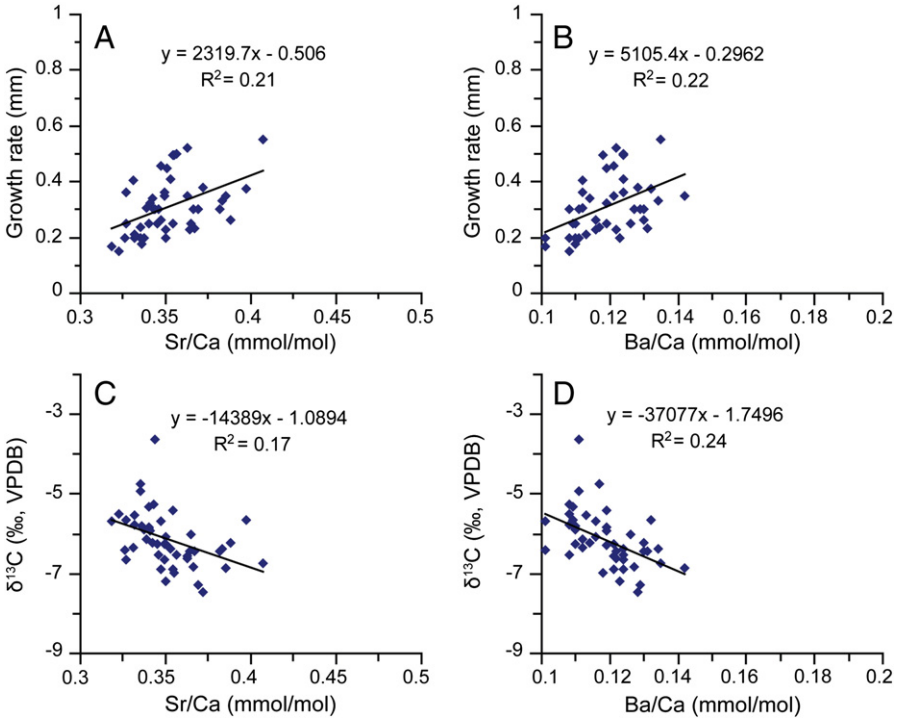


Figure 5. Correlations of (A) Sr/Ca vs growth rate, (B) Ba/Ca vs growth rate, (C) Sr/Ca vs $\delta^{13}C$, and (D) Ba/Ca vs $\delta^{13}C$ in stalagmite XL21. The growth rate and $\delta^{13}C$ series were interpolated to the chronology of the trace element series. The regression equations for each plot are shown.

the limestone host rock and the overlying soil layer during the past 95 years. The REE patterns of XL21, heavy REE-enrichment, and significantly positive Eu values, show broad similarities with that of the overlying soil (Fig. 6), suggesting that they were derived from REE leached from the overlying soil, in addition to bedrock-derived REE.

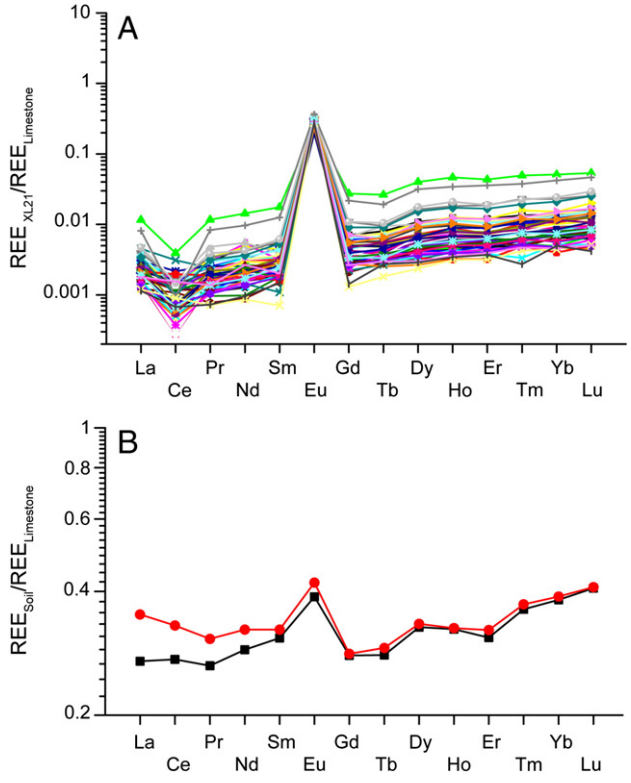


Figure 6. (A) REE series from stalagmite XL21 normalized against the host limestone. The colors represent different subsamples for REE analysis. (B) REE series from two subsamples of the overlying soil layer at Xianglong Cave normalized against the host limestone.

The positive Eu anomalies in XL21 are larger than those in the soil, and cannot be reproduced by simple mixing of the soil and limestone fractions. Although the REE generally show similar behaviors and are transported together through the environment, geochemical differences exist between the individual elements. For example, Ce and Eu commonly behave differently when compared with the other REE because of their greater sensitivity to changes in redox conditions (Henderson, 1984). Eu is the only lanthanide that, under reducing conditions, can be divalent, and is thus segregated from other REE under such conditions (Lee et al., 2003).

It has been suggested that divalent Eu is preferentially mobilized during water–rock interactions, and can contribute to Eu enrichment in streams (Leybourne and Johannesson, 2008) and groundwater (Guo et al., 2010). Thus, the explanation for the Eu enrichment recorded in stalagmite XL21 could be preferential mobilization of divalent Eu relative to the more particle-reactive trivalent REE from the soil overlying the cave. Negative Ce anomalies, similar to those observed in XL21, were also found in a stalagmite from southeastern France (Bourdin et al., 2011). It has been suggested that Ce anomalies in streams and groundwater (Smedley, 1991; Dia et al., 2000) are caused by the oxidative scavenging of tetravalent Ce by iron and/or manganese oxides (Ohta and Kawabe, 2001). As tetravalent Ce is more strongly adsorbed than the trivalent REE, the Ce oxidative scavenging reaction may result in negative Ce anomalies in seepage waters and speleothems.

Experimental studies suggest that the carbonate/water distribution factor for cations with ionic radii of <1 Å decreases when the crystallization rate of the carbonate mineral is high (Rimstidt et al., 1998). That means that small ions, like most REE (from Pr to Lu), are favored in speleothems during slow-growth periods (Bourdin et al., 2011). The positive correlation ($R = 0.44$, $N = 48$, $p < 0.01$) observed between the ΣREE/Ca and growth rate series in XL21 is contradictory to this growth-rate dependent model (Fig. 7). Figure 7 also shows consistent variations between the ΣREE/Ca ratio and temperature ($R = 0.40$, $N = 48$, $p < 0.01$), which is expected because the growth rate of XL21 was primarily controlled by temperature variations (Tan et al., 2013).

https://doi.org/10.1016/j.yqres.2013.12.001 Published online by Cambridge University Press

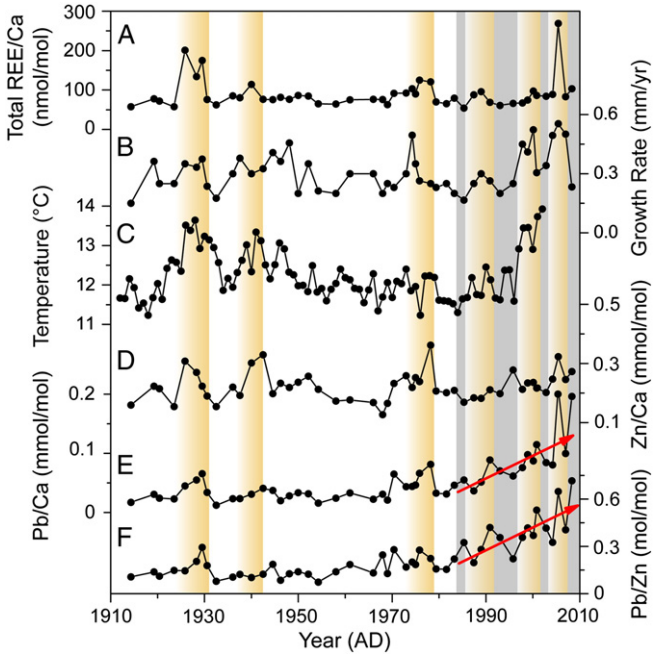


Figure 7. Comparisons of temporal variations in (A) ΣREE/Ca, with (B) stalagmite growth rate, (C) local temperature, and the (D) Zn/Ca, (E) Pb/Ca, and (F) Pb/Zn ratios from stalagmite XL21. The dark yellow bars mark periods showing good agreement among the different records. Red arrows indicate the continuous increasing trend of the Pb/Ca and Pb/Zn ratios since 1985, which suggests increasing mine-derived Pb pollution in the local environment over the past 30 yr (gray areas).

Fleet (1984) reported that a warm and humid climate would increase REE mobilization by weathering processes. A stalagmite from Songjia Cave in central China also showed that the REE concentrations were low during the last glacial maximum period, but significantly increased during the last deglaciation (Zhou et al., 2008).

Our results are consistent with previous studies (Richter et al., 2004; Zhou et al., 2008) and suggest that climate may affect REE concentrations in speleothems on decadal to annual timescales. Under a warm and humid climate, well-developed vegetation and enhanced microbial activity and organic decomposition in soil may enhance pCO_2 in the soil air, reduce the pH of the soil solution, and increase the concentration of organic matter in the soil (McCarthy et al., 1998; Spötl et al., 2005). These processes will increase REE mobilization from the overlying soil layer and the host rock of the cave, as well as transportation by groundwater, and ultimately increase the amounts preserved in speleothems. As there is plentiful rainfall in the Xianglong Cave area, temperature may be more dominant than precipitation in controlling REE variations in the groundwater and speleothems in this cave.

Controls on Zn and Pb variations in XL21

Good agreement was also observed among the Zn/Ca, Sr/Ca, Ba/Ca, and ΣREE/Ca ratios (Fig. 3). The correlation coefficient between Zn/Ca and Sr/Ca is 0.64 ($N = 48$, $p < 0.01$), and between Zn/Ca and ΣREE/Ca is 0.58 ($N = 48$, $p < 0.01$). The Zn/Ca ratios also show consistent variations with the growth rate ($R = 0.37$, $N = 48$, $p < 0.05$) and temperature ($R = 0.34$, $N = 48$, $p < 0.05$), which is as expected (Fig. 7).

Borsato et al. (2007) suggest that concentrations of Zn and Pb in speleothems can be attributed to transport in complexes with natural organic matter originating from the soil/epikarst above the cave. As discussed above, a warm and humid climate favors vegetation development and microbial activity, and can enhance organic decomposition in soil. As a result, higher temperatures may have increased the natural organic-matter mediated Zn mobilization from the epikarst above the cave, and led to increased Zn retention in stalagmite XL21.

The Pb/Ca ratio shows similar variations to Zn/Ca over annual timescale ($R = 0.45$, $N = 48$, $p < 0.01$). The peaks of Pb/Ca ratio, such as peaks at about AD 1930 and 1970s, are consistent with that of the Zn/Ca ratio before 1985 (Fig. 7), suggesting a common controlling factor. However, there is a notable increasing trend in the Pb/Ca ratio from 1985 onwards, which is not evident before this point (Fig. 7). As the geochemical characteristics and behavior of Pb and Zn are similar during deposition (Liu et al., 1984), we used the Pb/Zn ratio to study these anomalous Pb variations. Our results show that the Pb/Zn values are less than 0.3 mol/mol before 1985, but have shown a continual increase since then, with the highest value of 0.7 mol/mol occurring in 2008 (Fig. 7). This remarkable increasing trend in Pb/Zn is difficult to explain in terms of climate change. Instead, we believe that it records Pb pollution in this area.

Mining may cause heavy metal pollution of the atmosphere via the discharge of particulates and aerosols, and these pollutants may then be incorporated into soils by wet and dry atmospheric deposition (Pacyna et al., 2009). For example, peat bogs have recorded atmospheric pollution by lead and other heavy metals in Europe (Mighall et al., 2009). The lead mines around Xianglong Cave were first opened in 1984–1985, with an annual production of 200–240 tons. Since 1987, the construction of mechanized production lines has increased the output of lead dramatically to 6000–8000 tons/yr (personal communication with the ex-director of the mine, Mr. S. Liu in 2012). During winter, the predominantly northwesterly winds carry mine-derived dust (Wei et al., 2000) that is deposited and subsequently washed into the karst system. We infer that it was this atmospheric lead pollution that was recorded in the speleothem. The increasing trend of Pb/Zn in XL21 after the mid-1980s is consistent with the enhanced lead production, suggesting an increase in mine-derived Pb pollution in the local environment over the past 30 years.

Conclusions

(1) The Sr/Ca and Ba/Ca ratios in stalagmite XL21 show a significant positive correlation and were primarily controlled by growth rate. As temperature influences the production of soil CO_2, affecting the leaching of soil cations and carbonate dissolution, and controlling growth rate variability, it could also have had an indirect effect on variations in the Sr and Ba levels of XL21.

(2) The REE patterns of XL21, HREE-enrichment and significantly positive Eu values, show broad similarities with the overlying soil, indicating that they were derived from REE leached from the overlying soil, in addition to bedrock-derived REE. Temperature affected the REE concentrations in XL21 over decadal to annual timescales during the past 95 years, by controlling pCO_2, pH, and the concentration of organic matter in the soil, and consequently affecting REE mobilization from the overlying soil layer and the host rock.

(3) The concentration of Zn in XL21 was affected by the mobile organic matter in the overlying soil layer above the cave, which was influenced by temperature. Higher temperatures encourage increased vegetation cover and microbial activity, which enhanced the mobilization of the natural organic matter from the epikarst zone above the cave and caused an increase in Zn retention by XL21.

(4) The Pb/Ca ratio in the stalagmite shows an anomalously increasing trend since 1985, which is consistent with enhanced lead production in this area, and indicates an increase in mine-derived Pb pollution in the local environment over the past 30 years.

Acknowledgments

We acknowledge A. Osincev, S. Breitenbach and H. Zhang for surveying and drawing the cave. The final version of the manuscript benefited

for constructive suggestions from two anonymous reviewers and Prof. Alan Gillespie and Prof. John Dodson. This work was supported by the National Basic Research Program of China (grant 2013CB955902; 2010CB833405); Key Program of the Chinese Academy of Sciences (grant KZZD-EW-04-01); and National Science Foundation of China (grant 41023006; 41230524; 41001061; 41372192). We also thank financial supported by Taiwan NSC (98-2116-M002-012, 99-2628-M002-012, 99-2611-M002-005, and 100-3113-M-002-002 to CCS) and National Taiwan University (101R7625 to CCS).

References

Ayalon, A., Bar-Matthews, M., Kaufman, A., 1999. Petrography, strontium, barium and uranium concentrations, and strontium and uranium isotope ratios in speleothems as palaeoclimatic proxies: Soreq Cave, Israel. The Holocene 9, 715–722.

Borsato, A., Frisia, S., Fairchild, I.J., Somogyi, A., Susini, J., 2007. Trace element distribution in annual stalagmite laminae mapped by micrometer-resolution X-ray fluorescence: implications for incorporation of environmentally significant species. Geochimica et Cosmochimica Acta 71, 1494–1512.

Bourdin, C., Douville, E., Genty, D., 2011. Alkaline-earth metal and rare-earth element incorporation control by ionic radius and growth rate on a stalagmite from the Chauvet Cave, Southeastern France. Chemical Geology 290, 1–11.

Cai, Y., Zhang, H., Cheng, H., An, Z., Lawrence Edwards, R., Wang, X., Tan, L., Liang, F., Wang, J., Kelly, M., 2012. The Holocene Indian monsoon variability over the southern Tibetan Plateau and its teleconnections. Earth and Planetary Science Letters 335–336, 135–144.

Chen, H., Zheng, C., Tu, C., Zhu, Y., 1999. Heavy metal pollution in soils in China: status and countermeasures. Ambio 28, 130–134.

Cheng, S., 2003. Heavy metal pollution in China: origin, pattern and control. Environmental Science and Pollution Research 10, 192–198.

Cheng, H., Edwards, R.L., Broecker, W.S., Denton, G.H., Kong, X., Wang, Y., Zhang, R., Wang, X., 2009. Ice age terminations. Science 326, 248–252.

Cheng, H., Lawrence Edwards, R., Shen, C.-C., Polyak, V.J., Asmerom, Y., Woodhead, J., Hellstrom, J., Wang, Y., Kong, X., Spötl, C., Wang, X., Calvin Alexander Jr., E., 2013. Improvements in ^{230}Th dating, ^{230}Th and ^{234}U half-life values, and U–Th isotopic measurements by multi-collector inductively coupled plasma mass spectrometry. Earth and Planetary Science Letters 371–372, 82–91.

Cruz, J.F.W., Burns, S.J., Jercinovic, M., Karmann, I., Sharp, W.D., Vuille, M., 2007. Evidence of rainfall variations in Southern Brazil from trace element ratios (Mg/Ca and Sr/Ca) in a Late Pleistocene stalagmite. Geochimica et Cosmochimica Acta 71, 2250–2263.

Dia, A., Gruau, G., Olivié-Lauquet, G., Riou, C., Molénat, J., Curmi, P., 2000. The distribution of rare earth elements in groundwaters: assessing the role of source-rock composition, redox changes and colloidal particles. Geochimica et Cosmochimica Acta 64, 4131–4151.

Edwards, R.L., Chen, J.H., Wasserburg, G.J., 1987. ^{238}U–^{234}U–^{230}Th–^{232}Th systematic and the precise measurement of time over the past 500,000 years. Earth and Planetary Science Letters 81, 175–192.

Fairchild, I.J., Treble, P.C., 2009. Trace elements in speleothems as recorders of environmental change. Quaternary Science Reviews 28, 449–468.

Fairchild, I.J., Borsato, A., Tooth, A.F., Frisia, S., Hawkesworth, C.J., Huang, Y., McDermott, F., Spiro, B., 2000. Controls on trace element (Sr–Mg) compositions of carbonate cave waters: implications for speleothem climatic records. Chemical Geology 166, 255–269.

Fairchild, I.J., Smith, C.L., Baker, A., Fuller, L., Spotl, C., Mattey, D., McDermott, F., E.I.M.F., 2006. Modification and preservation of environmental signals in speleothems. Earth Science Reviews 75, 105–153.

Finch, A.A., Shaw, P.A., Weedon, G.P., Holmgren, K., 2001. Trace element variation in speleothem aragonite: potential for palaeoenvironmental reconstruction. Earth and Planetary Science Letters 186, 255–267.

Fleet, A.J., 1984. Aqueous and sedimentary geochemistry of rare earth elements. In: Henderson, J. (Ed.), Rare Earth Element Geochemistry. Elsevier, Oxford, pp. 343–373.

Fleitmann, D., Burns, S.J., Mudelsee, M., Neff, U., Kramers, J., Mangini, A., Matter, A., 2003. Holocene forcing of the Indian monsoon recorded in a stalagmite from southern Oman. Science 300, 1737–1739.

Frisia, S., Borsato, A., Fairchild, I.J., Susini, J., 2005. Variations in atmospheric sulphate recorded in stalagmites by synchrotron micro-XRF and XANES analyses. Earth and Planetary Science Letters 235, 729–740.

Goede, A., McCulloch, M., McDermott, F., Hawkesworth, C., 1998. Aeolian contribution to strontium and strontium isotope variations in a Tasmanian speleothem. Chemical Geology 149, 37–50.

Guo, H., Zhang, B., Wang, G., Shen, Z., 2010. Geochemical controls on arsenic and rare earth elements approximately along a groundwater flow path in the shallow aquifer of the Hetao Basin, Inner Mongolia. Chemical Geology 270, 117–125.

Hellstrom, J., McCulloch, M., 2000. Multi-proxy constraints on the climatic significance of trace element records from a New Zealand speleothem. Earth and Planetary Science Letters 179, 287–297.

Henderson, P., 1984. General geochemical properties and abundances of the rare earth elements. In: Henderson, P. (Ed.), Rare Earth Element Geochemistry. Elsevier, Oxford, pp. 1–32.

Hori, M., Ishikawa, T., Nagaishi, K., Lin, K., Wang, B.-S., You, C.-F., Shen, C.-C., Kano, A., 2013. Prior calcite precipitation and source mixing process influence Sr/Ca, Ba/Ca and 87Sr/86Sr of a stalagmite developed in southwestern Japan during 18.0–4.5 ka. Chemical Geology 347, 190–198.

Huang, C., Gong, Z., 2001. Geochemical implication of rare earth elements in process of soil development. Journal of Rare Earths 19, 57–62.

Johnson, K.R., Hu, C., Belshaw, N.S., Henderson, G.M., 2006. Seasonal trace-element and stable-isotope variations in a Chinese speleothem: the potential for high-resolution. Earth and Planetary Science Letters 244, 394–407.

Karmann, I., Cruz Jr., F.W., Viana Jr., O., Burns, S.J., 2007. Climate influence on geochemistry parameters of waters from Santana–Pérolas cave system, Brazil. Chemical Geology 244, 232–247.

Lee, S.-G., Lee, D.-H., Kim, Y., Chae, B.-G., Kim, W.-Y., Woo, N.-C., 2003. Rare earth elements as indicators of groundwater environment changes in a fractured rock system: evidence from fracture-filling calcite. Applied Geochemistry 18, 135–143.

Leybourne, M.I., Johannesson, K.H., 2008. Rare earth elements (REE) and yttrium in stream waters, stream sediments, and Fe–Mn oxyhydroxides: fractionation, speciation, and controls over REE + Y patterns in the surface environment. Geochimica et Cosmochimica Acta 72, 5962–5983.

Liu, Y., Cao, L., Wang, H., Chu, T., Zhang, J., 1984. Element Geochemistry. Science Press, Beijing (In Chinese).

Liu, X., Fang, J., Yang, X., Li, X., 2003. Climatology of dekadly precipitation around the Qinling mountains and characteristics of its atmospheric circulation. Arid Meteorology 21, 8–13 (in Chinese with English abstract).

Lo, L., X., Shen, C.-C., Lu, C.-J., Chen, Y.-C., Chang, C.-C., Wei, K.-Y., Qu, D., Gagan, M.K., 2013. Determination of element/Ca ratios in foraminifera and corals using cold- and hot-plasma techniques in inductively coupled plasma sector field mass spectrometry. Journal of Asian Earth Sciences. http://dx.doi.org/10.1016/j.jseaes.2013.11.016 (in press).

Lorens, R.B., 1981. Sr, Cd, Mn and Co distribution coefficients in calcite as a function of calcite precipitation rate. Geochimica et Cosmochimica Acta 45, 553–561.

McCarthy, J.F., Sanford, W.E., Stafford, P.L., 1998. Lanthanide field tracers demonstrate enhanced transport of transuranic radionuclides by natural organic matter. Environmental Science & Technology 32, 3901–3906.

McDermott, F., 2004. Palaeo-climate reconstruction from stable isotope variations in speleothems: a review. Quaternary Science Reviews 23, 901–918.

Mighall, T., Timberlake, S., Foster, I.D., Krupp, E., Singh, S., 2009. Ancient copper and lead pollution records from a raised bog complex in Central Wales, UK. Journal of Archaeological Science 36, 1504–1515.

Musgrove, M., Banner, J.L., 2004. Controls on the spatial and temporal variability of vadose dripwater geochemistry: Edwards Aquifer, central Texas. Geochimica et Cosmochimica Acta 68, 1007–1020.

Ohta, A., Kawabe, I., 2001. REE(III) adsorption onto Mn dioxide and Fe oxyhydroxide: Ce(III) oxidation by Mn dioxide. Geochimica et Cosmochimica Acta 65, 695–703.

Pacyna, J.M., Pacyna, E.G., Aas, W., 2009. Changes of emissions and atmospheric deposition of mercury, lead, and cadmium. Atmospheric Environment 43, 117–127.

Richter, D.K., Gotte, T., Niggemann, S., Wurth, G., 2004. REE^{3+} and Mn^{2+} activated cathodoluminescence in lateglacial and Holocene stalagmites of central Europe: evidence for climatic processes? The Holocene 14, 759–767.

Rimstidt, J.D., Balog, A., Webb, J., 1998. Distribution of trace elements between carbonate minerals and aqueous solutions. Geochimica et Cosmochimica Acta 62, 1851–1863.

Roberts, M.S., Smart, P.L., Baker, A., 1998. Annual trace element variations in a Holocene speleothem. Earth and Planetary Science Letters 154, 237–246.

Shen, C.-C., Wu, C.-C., Liu, Y., Yu, J., Chang, C.-C., Lam, D.D., Chou, C.-J., Lo, L., Wei, K.-Y., 2011. Measurements of natural carbonate rare earth elements in femtogram quantities by inductive coupled plasma sector field mass spectrometry. Analytical Chemistry 83, 6842–6848.

Shen, C.-C., Wu, C.-C., Cheng, H., Lawrence Edwards, R., Hsieh, Y.-T., Gallet, S., Chang, C.-C., Li, T.-Y., Lam, D.D., Kano, A., Hori, M., Spötl, C., 2012. High-precision and high-resolution carbonate 230Th dating by MC-ICP-MS with SEM protocols. Geochimica et Cosmochimica Acta 99, 71–86.

Siklosy, Z., Kern, Z., Demeny, A., Pilet, S., Leel-Ossy, S., Lin, K., Shen, C.-C., Szeles, E., Breitner, D., 2011. Speleothems and pine trees as sensitive indicators of environmental pollution—a case study of the effect of uranium-ore mining in Hungary. Applied Geochemistry 26, 666–678.

Smedley, P.L., 1991. The geochemistry of rare earth elements in groundwater from the Carnmenellis area, southwest England. Geochimica et Cosmochimica Acta 55, 2767–2779.

Spötl, C., Fairchild, I.J., Tooth, A.F., 2005. Cave air control on dripwater geochemistry, Obir Caves (Austria): implications for speleothem deposition in dynamically ventilated caves. Geochimica et Cosmochimica Acta 69, 2451–2468.

Stoll, H., Muller, W., Prieto, M., 2012. I-STAL, a model for interpretation of Mg/Ca, Sr/Ca and Ba/Ca variations in speleothems and its forward and inverse application on seasonal to millennial scales. Geochemistry, Geophysics, Geosystems 13. http://dx.doi.org/10.1029/2012GC004183.

Tan, L., Yi, L., Cai, Y., Shen, C.-C., Cheng, H., An, Z., 2013. Quantitative temperature reconstruction based on growth rate of annually-layered stalagmite: a case study from central China. Quaternary Science Reviews 72, 137–145.

Tesoriero, A.J., Pankow, J.F., 1996. Solid solution partitioning of Sr^{2+}, Ba^{2+}, and Cd^{2+} to calcite. Geochimica et Cosmochimica Acta 60, 1053–1063.

Treble, P., Shelley, J.M.G., Chappell, J., 2003. Comparison of high resolution sub-annual records of trace elements in a modern (1911–1992) speleothem with instrumental

climate data from southwest Australia. Earth and Planetary Science Letters 216, 141–153.
Treble, P.C., Chappell, J., Shelley, J.M.G., 2005. Complex speleothem growth processes revealed by trace element mapping and scanning electron microscopy of annual layers. Geochimica et Cosmochimica Acta 69, 4855–4863.
Wang, Y., Cheng, H., Edwards, R.L., An, Z.S., Wu, J.Y., Shen, C.-C., Dorale, J.A., 2001. A high-resolution absolute-dated late Pleistocene Monsoon record from Hulu cave, China. Science 294, 2345–2348.
Wang, Y., Cheng, H., Edwards, R.L., He, Y., Kong, X., An, Z., Wu, J., Kelly, M.J., Dykoski, C.A., Li, X., 2005. The Holocene Asian monsoon: links to solar changes and North Atlantic climate. Science 308, 854–857.
Wang, Y., Cheng, H., Edwards, R.L., Kong, X., Shao, X., Chen, S., Wu, J., Jiang, X., Wang, X., An, Z., 2008. Millennial- and orbital-scale changes in the East Asian monsoon over the past 224,000 years. Nature 451, 1090–1093.
Wei, Y., Huang, C., Sun, G., 2000. Study on the Holocene loess sedimentary stratigraphy in Hanzhong basin. Arid Land Geography 23, 37–43 (In Chinese with English abstract).
Wong, C.I., Banner, J.L., Musgrove, M., 2011. Seasonal dripwater Mg/Ca and Sr/Ca variations driven by cave ventilation: implications for and modeling of speleothem paleoclimate records. Geochimica et Cosmochimica Acta 75, 3514–3529.
Yuan, D., Cheng, H., Edwards, R.L., Dykoski, C.A., Kelly, M.J., Zhang, M., Qing, J., Lin, Y., Wang, Y., Wu, J., Dorale, J.A., An, Z., Cai, Y., 2004. Timing, duration, and transitions of the Last Interglacial Asian Monsoon. Science 304, 575–578.
Zhou, H., Chi, B., Lawrence, M., Zhao, J., Yan, J., Greig, A., Feng, Y., 2008. High-resolution and precisely dated record of weathering and hydrological dynamics recorded by manganese and rare-earth elements in a stalagmite from Central China. Quaternary Research 69, 438–446.
Zhou, H., Feng, Y.-x, Zhao, J.-x, Shen, C.-C., You, C.-F., Lin, Y., 2009. Deglacial variations of Sr and $^{87}Sr/^{86}Sr$ ratio recorded by a stalagmite from Central China and their association with past climate and environment. Chemical Geology 268, 233–247.
Zhou, H., Greig, A., Tang, J., You, C.-F., Yuan, D., Tong, X., Huang, Y., 2012. Rare earth element patterns in a Chinese stalagmite controlled by sources and scavenging from karst groundwater. Geochimica et Cosmochimica Acta 83, 1–18.

https://doi.org/10.1016/j.yqres.2013.12.001 Published online by Cambridge University Press